Compressibility and Drained Shear Characteristics of a Sand under High Confining Pressures

Norihiko MIURA* and Toyotoshi YAMANOUCHI**

(Received August 31, 1973)

Abstract

The compressibility and drained shear characteristics of a sand under high pressures were investigated. A particular relationship was found between degree of compression, isotropic pressure and compression time, for a certain range of pressures. At a pressure higher than 300 kg/sq. cm, however, the time necessary to reach 100 per cent compression was so long that it could not be attained the final stage of a long-term compression test extending over several hundred hours.

The shear characteristics of the sand tested was found to be affected by the initial void ratio at a confining pressure as high as 500 kg/sq. cm. It was shown that the shear characteristics of a sand under high confining pressures was significantly influenced not only by the phenomenon of grain crushing but also by the action of pore water.

Introduction

The mechanical properties of soils under high pressure have been observed since the earliest days of soil mechanics. Recently, the importance of studying the high pressure characteristics of soils has become widely recongnized, especially with regard to the construction of large-scale fill dams and the bearing capacity of piles.

From a civil engineering viewpoint, the range of pressures to be considered may be as high as several hundred kg/sq. cm. A number of investigations of the mechanical properties of soils subject to high pressures have been made using an elevated-cell pressure apparatus, however, not much data has been presented for pressures higher than 200 kg/sq. cm. According to these limited data, we know that the mechanical properties of a soil at high pressure must be distinguished from those of a soil at lower confining pressures. Also, the high pressure properties of a soil have a significant relation to the phenomenon of the crushing of soil grains. However, much more data is needed in order to obtain a sufficient understanding of the high pressure behavior of soils.

In order to know how the initial porosity affects the mechanical properties of a sand for an increase of confining pressure, the authors carried out a series of drained triaxial compression tests under various confining pressures up to 500 kg/sq. cm. The effect of pore water on the mechanical properties of a sand under high pressure was also investigated.

* Department of Civil Engineering.

** Department of Civil Engineering, Faculty of Engineering, Kyushu University.

High Pressure Apparatus

The essential features of the high pressure apparatus used in this study are not so different from those of a standard apparatus. Since the apparatus was operated under high pressures, however, the following aspects were revised: *Sealing*; In order to seal high pressures, O-rings were used where required. A special O-ring of low friction was prepared for sealing such movable parts as the piston and the pressure accumulator. The piston friction was mostly eliminated by subtracting the piston friction, which was determined in preliminary test, from the measured axial compression load. The magnitude of the piston friction for various confining pressures was as shown in Fig. 1. *Membrane*; A rubber

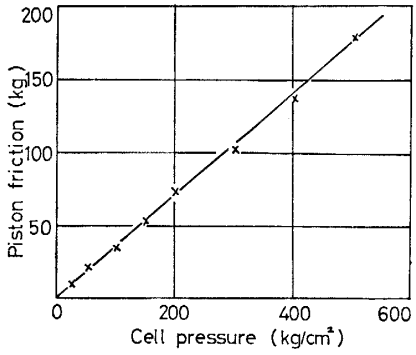

Fig. 1. Piston friction.

membrane of about 1 mm thick was used. It was confirmed that no leakage occurred through the membrane during the high confining pressure tests. In calculating deviator stresses, it was assumed that the strength of the membrane could be neglected. *Cell pressure*; A high cell pressure was generated by an air-hydraulic pump, and it was maintained and regulated by means of a pressure accumulator. Throughout the tests, the confining pressure could be maintained reasonably constant, with the variation being ± 0.3 per cent of any confining pressure. Water, to which was added some amount of antirust agent, was used as the pressure medium. The high pressure apparatus is shown in Fig. 2.

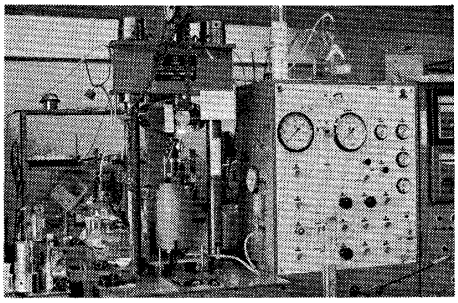

Fig. 2. High-pressure supplying apparatus.

Samples and Their Preparations

All tests were conducted on so-called "Toyoura standard sand." This sand consists mostly of quartz (70%), chert (8%) and feldspar (22%), with grains shapes from subangular to subrounded. The main characteristics of the sand are as follows: Uniformity coefficient: 1.5, specific gravity: 2.646, maximum void ratio: 0.91, minimum void ratio: 0.58, maximum porosity: 47.6%, and minimum porosity: 36.7%.

The dense state specimens were prepared by tamping the desiccator-dried sand in 16 layers using a rubber-tipped tamper. They were saturated afterwards, by acting vacuum on the top of sample and then supplementing de-aired water at the bottom of it. Most of the samples obtained with the above-mentioned procedure had void ratios of from 0.60 to 0.62. The loose state saturated specimens were prepared by spooning the submerged sand into the rubber membrane which was filled with de-aired water. The loose state dry specimens were made by pouring desiccator-dried sand through a funnel. Both procedures produced samples with void ratios of from 0.82 to 0.84 in most cases.

Tests

Drained shear tests, so-called "CD tests," were performed at various confining pressures up to 500 kg/sq. cm. For the samples which were confined at pressures lower than 200 kg/sq. cm, enough time was permitted to achieve 100 per cent compression. In tests at pressures higher than 300 kg/sq. cm, 100 per cent compression of samples could not be attained even after several hours, and it was pressumed that it might require more than several hundred hours to reach the final stage of compression. In those tests, compression was stopped when the rate of volume change of the samples had decreased to a value of 0.1 cu. cm/hr. In order to know the time necessary to attain complete compression under high pressures, another series of long-term isotropic compression tests were programmed. A couple of long-term compression tests were tried at pressures of 300 and 500 kg/sq. cm, but neither test could be completed, since it was found in both tests that the pressure gage was no longer calibrated after long continuous running. However, it was found that 100 per cent compression could not be reached before 350 or 570 hours for a dense specimen compressed isotropically at a pressure of 300 or 500 kg/sq. cm.

The rate of strain was 0.25 per cent of the specimen height per minute when a specimen was sheared at the confining pressures higher than 250kg/sq. cm, and 0.5 per cent/min at the confining pressures lower than 250kg/sq. cm. It was confirmed that no excess pore pressure occurred during tests at the above-mentioned strain rates. The axial strain, to which most of the specimens were subjected, was 40 per cent of their original height, which corresponds to a natural strain

of about 51 per cent. The shape of the specimen was nearly cylindrical even after it had been strained considerably, as is illustrated in Fig. 3. Then, a correc-

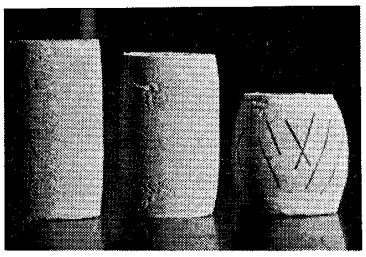

Fig. 3. Shapes of the specimens after triaxial tests. Axial strain of each sample is, from the left towards the right, 20, 30 and 45 per cent of each original height. Multiple failure lines of the last specimen were traced in ink.

tion of the cross-sectional area of the specimen was made assuming that the shape of the sample remained cylindrical throughout the test. The axial compression load was measured by a probing ring whose capacity was 50 tons. It was assumed that the volume change of a saturated sample is indicated by the volume of water draining into an open buret which was connected to the sample. To be exact, volume changes measured in this way do not indicate the true volume change of the sample, because the measured value includes the volume that the membrane penetrates into the spaces of the sand. However, reliable information from the volume of membrane penetration could not be obtained. The volume change of the dry sample was also measured using a closed buret after Bishop and Henkel.[1] The values measured in these tests were all recorded automatically on a chart.

Compressibility of Sand

When the applied isotropic pressure was lower than 200 kg/sq. cm, the sand samples reached 100 per cent compression in a few hours. The curves showing the relation between isotropic pressure and time necessary to reach the ultimate compression are shown in Fig. 4.

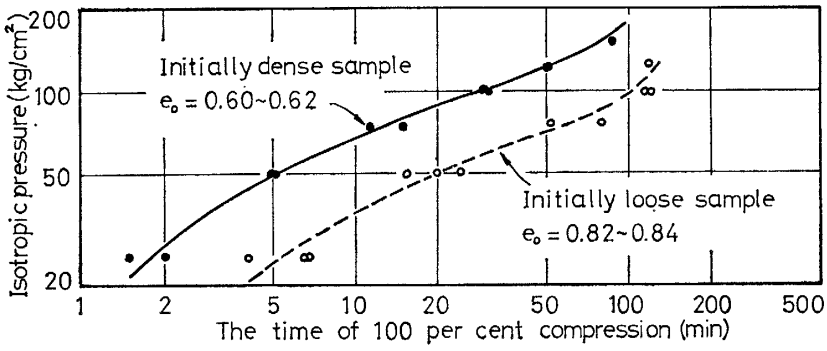

Fig. 4. Time necessary to reach 100 per cent compression in function of isotropic pressure.

In the case of the saturated samples, the relationships between degree of compression U and logarithm of the compression time are shown in Fig. 5, for

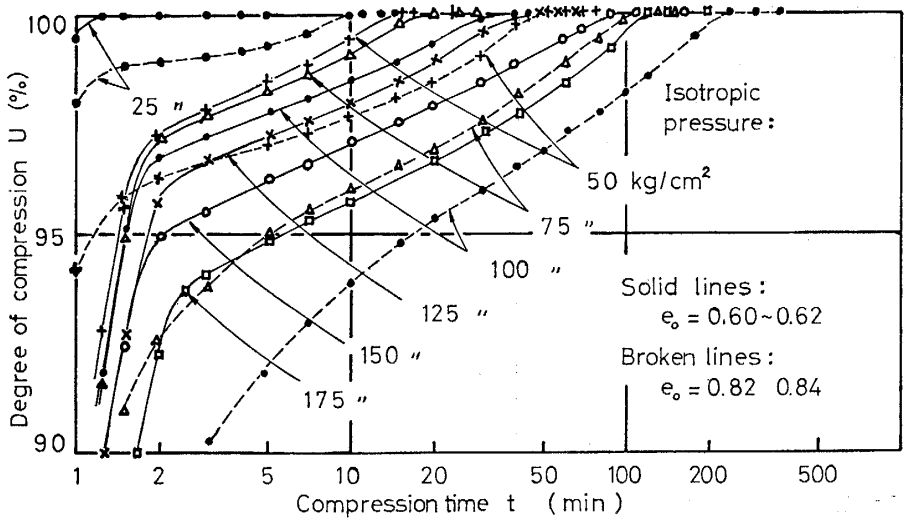

Fig. 5. Relationship between degree of compression and compression time.

several pressures up to 175 kg/sq. cm. Most of these curves show a particular shape, for which we find that the line between the two reflection points is approximately straight. In addition, all of these curves rise a little just before the termination of compression. Hence, we can estimate the time necessary to reach 100 per cent compression by extrapolating the straight line. Consequently, there exists a relationship between degree of compression, pressure, and compression time, as follows:

$$100-U_{tx}=a\log_{10}(t_{100}/t_x)$$

or

$$t_{100}=t_x\cdot\exp\left(\frac{100-U_{tx}}{0.434a}\right) \qquad \cdots\cdots\cdots(1)$$

where, $U_{tx}(\%)$ is the degree of compression when $t=t_x(\text{min})$, t_{100} is the time necessary to reach 100 per cent compression, and a is the slope of straight line. U_{tx} and a are functions of pressure which can be determined experimentally. For the sand tested, the values of U_{tx} and a are those given in Fig. 6 and Table 1.

Under higher isotropic pressures, the compression of the saturated samples continued for a fairly-long time, and the porosity of the sand decreased considerably, as shown in Fig. 7. By letting e_0 be the initial void ratio, e_{10} be the void ratio after 10 hours of compression, and e_{ft} be the final void ratio of the tested sample, the authors formulated the following equation,

$$\frac{e_{10}-e_{ft}}{e_0-e_{10}}=C \qquad \cdots\cdots\cdots(2)$$

Referring to Fig. 7, the C values obtained for 200 L, 300 D, 300 L and 500 D are 0.22, 0.22, 0.19 and 0.52, respectively. If the compression tests had been continued further, larger values of void ratios e_{ft} for the samples would have

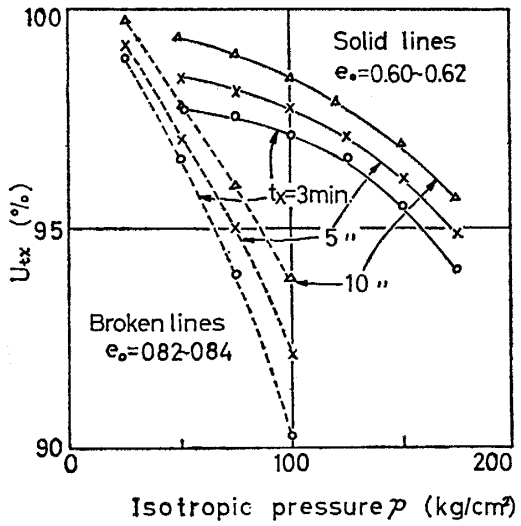

Fig. 6. Values of U_{tx}.

Table 1. Values of a.

Initial void ratio	Isotropic compression pressures 25 (kg/cm²)	50 (〃)	75 (〃)	100 (〃)	125 (〃)	150 (〃)	175 (〃)
0.60–0.62	—	2.78	2.80	2.60	2.57	2.79	3.15
0.82–0.84	1.48	2.65	3.19	4.08	—	—	—

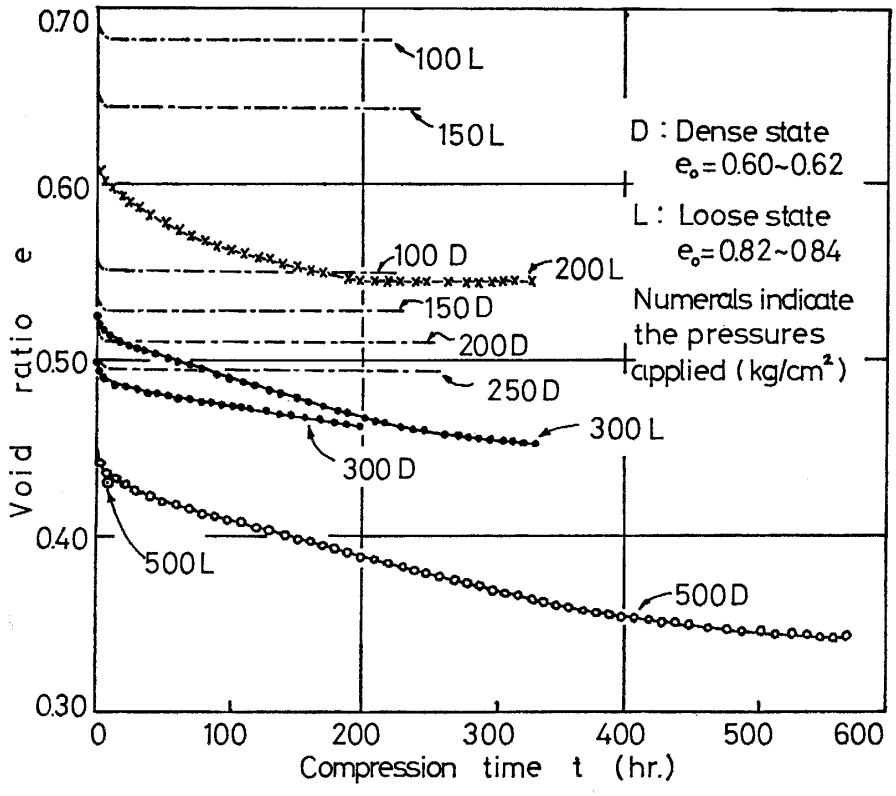

Fig. 7. Curves of long-term compression under high isotropic pressures in saturated samples.

been attained, except for the sample 200 L which seems to have attained the ultimate compression. Thus, by substituting an ultimate void ratio e_f into Eq. (2) instead of e_{ft}, some relationships between pressure and value of C will be obtained. The experimental results mentioned above indicate that the porosity of a sand under high pressure is affected not only by the magnitude of that pressure but also by its duration.

Table 2. Gradings of the samples after compression under isotropic pressures.

Test No.	Applied pressure (kg/cm²)	Initial density	Moisture condition	Compression time	Per cent finer by weight				
					250μ	177μ	149μ	105μ	74μ
Untested sand					92.0	18.9	3.4	0.4	0.1
HD- 97	500	Dense	Sat*	570 hr.	94.0	45.6	27.0	17.6	11.7
HD- 31	500	Dense	Sat	7 hr.	93.5	40.9	22.1	13.7	8.8
HL- 30	500	Loose	Sat	16 hr.	94.7	49.7	30.5	20.1	13.5
HD- 99	500	Dense	Dry	20 hr.	92.2	33.3	15.6	8.9	5.4
HD- 94	300	Dense	Sat	205 hr.	92.9	31.1	11.6	5.6	3.1
HD- 32	300	Dense	Sat	9 hr.	92.8	29.7	12.3	6.3	3.6
HD-107	300	Dense	Sat	5 min.	91.9	23.9	7.8	3.4	1.8
HL- 95	300	Loose	Sat	330 hr.	94.0	43.8	24.3	14.6	9.1
HL-102	300	Loose	Sat	45 hr.	94.2	42.9	24.3	14.9	9.4
HL-108	300	Loose	Sat	5 min.	93.7	35.6	16.7	8.9	5.2
HD- 98	300	Dense	Dry	56 hr.	92.2	27.7	8.3	3.5	1.8
HD- 33	200	Dense	Sat	7 hr.	92.3	25.5	6.9	2.5	1.2
HD-106	200	Dense	Sat	3 min.	91.6	21.6	5.2	1.5	0.7
HL-104	200	Loose	Sat	327 hr.	94.5	39.0	20.5	11.6	6.9
HL-109	200	Loose	Sat	3 min.	93.4	29.0	11.3	5.3	2.9
HD-100	200	Dense	Dry	23 hr.	91.6	23.2	5.1	1.5	0.7
HD- 34	100	Dense	Sat	9 hr.	91.8	21.6	3.9	0.7	0.3
HD-105	100	Dense	Sat	2 min.	91.9	22.1	3.8	0.6	0.2
HL-101	100	Loose	Sat	5 hr.	91.3	22.8	6.2	2.1	1.0

* Sat: Saturated.

The gradings of the samples after compression are given in Table 2. It was thereby found that the greater part of the crushing of sand grains has been attained until the initial reflection point, which appeared in the curves of the degree of compression as a function of compression time shown in Fig. 5. The higher the applied pressure, the larger becomes the amount of grain crushing after the initial reflection point. The initial reflection point may be said to be such a significant one, that the average intergranular pressure becomes nearly equal to the average breakdown strength of the grains, as a result of primary crushing of the grains. After the initial reflection point, compression results mainly from intergranular slide.

For the dry samples, the relationships between void ratio and compression time are those shown in Fig. 8. It is obvious that pore water has no influence on the compressibility of the sand at pressures up to 200 kg/sq. cm, as compared with the results given in Fig. 7. However, the effect of pore water on the com-

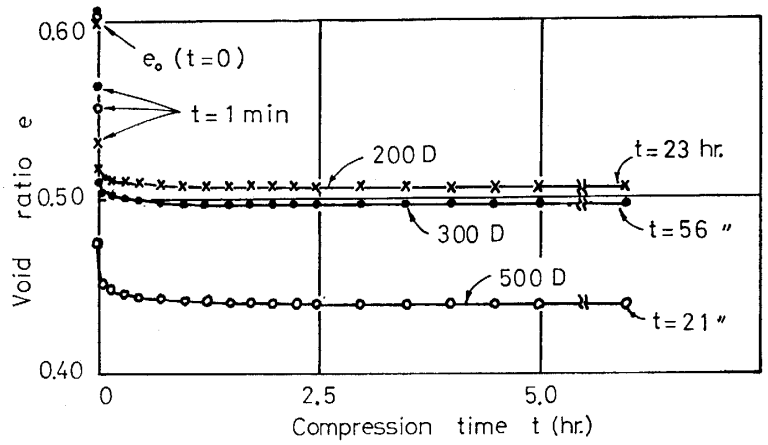

Fig. 8. Results of long-term compression tests under high isotropic pressures in dry samples.

pressibility of the sand is considerably large when the applied pressure is higher than 300 kg/sq. cm. It may be said that the dissolution of silica at the contact parts of the grains is related to the effect of water on the compressibility of the sand.

Curves showing the void ratio of the samples tested at various isotropic pressures are presented in Fig. 9. In the diagram, the broken line indicates

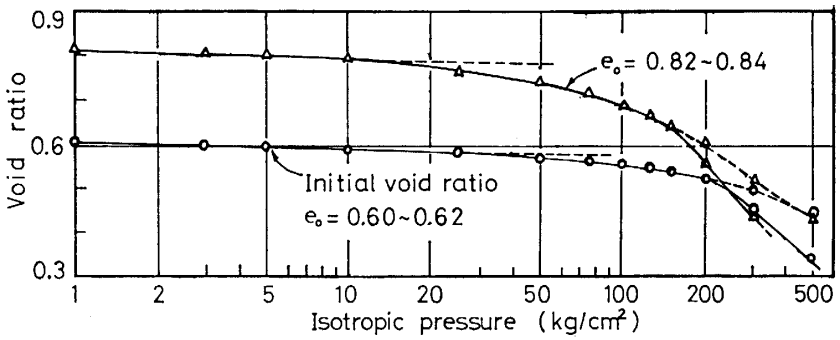

Fig. 9. Relation curves between void ratio and isotropic pressure.

the results of several hours of compression tests, and solid line shows the results of long-term compression tests. It is noted that the two curves given in Fig. 9 are approximately straight and are also parallel each other, throughout a certain range of pressures. Furthermore, both straight lines indicate a very small compressibility index of 0.02. These findings suggest that a loose state granular material can bear a considerably high pressure with only a small decrease of porosity. Hence, it appears that granular materials in the lower part of a fill dam can not be expected to be further compacted by the weight of the materials of the upper part of the dam to be surcharged later. Furthermore, the granular material of such a state may be lost its stability as the result of a dynamic force. Therefore, it is recommended that the materials of the lower part of a fill dam be compacted as much as possible at the time of construction, especially for stability against earthquakes.

It can be seen from Fig. 9 that the slopes of the curves change at a relatively high pressure, and that for the pressures higher than those reflection point, the slopes of the curves become considerably steep. The change of slope of the curve indicates an abrupt change of the crushing effect of the sand grains, as illustrated in Fig. 10. It is noted that a sand has a high compressibility index C_c as a result

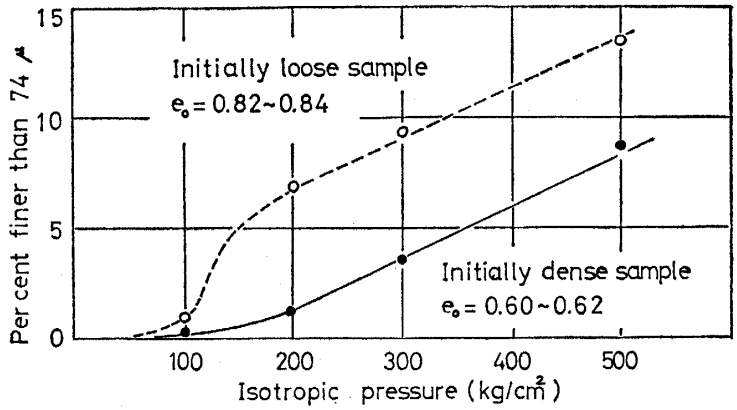

Fig. 10. Curves showing the change of crushing effect with increasing of isotropic pressure.

of the above-mentioned grain crushing phenomenon. For the sand used in this study, the values of C_c in the high pressure range were 0.25 and 0.52 for dry and saturated conditions, respectively. The void ratios of the two samples, which were of initially different porosities, approached a certain value at the reasonably high pressure of 500 kg/sq. cm. However, it should be noted that the crushing effect on the initially loose state sample was larger than that on the initially dense state one, as is seen in Table 2.

Shear Characteristics

The results of drained shear tests at various confining pressures are given in Tables 3 and 4. The relationships between deviator stress, axial strain (natural) and volumetric strain (natural) of these samples are also shown in Figs. 11 to 13.

At a confining pressure of 25 kg/sq. cm, the slopes of the curves are essentially similar to those obtained at relatively low pressures. For the dense samples, the confining pressure for which no volume change occurs at failure was interpolated to be 40 kg/sq. cm. At a pressure of 75 kg/sq. cm, the maximum deviator stress of the loose state sample attained the same value as that of the dense state one. For these samples, the rate of decrease of the porosity of the loose state sample was found to be larger than that of the dense state sample during shear, as can be seen in Table 3. These stress-strain relations can not be explained by the stress dilatancy theory,[2] because the theory does not take account of the volume change due to grain crushing. However, comparative

Table 3. Results of triaxial tests at constant cell pressures on saturated samples.

Test No.	Confining pressure	Initial void ratio	Void ratio after compression	Volumetric strain due to compression	Axial strain due to compression	Values at the time of failure: Deviator stress	Axial strain	Volumetric strain	Void ratio	Mean normal stress	Principal stress ratio	Secant angle	Dilatancy rate
	(kg/cm²)			(%)	(%)	(kg/cm²)	(%)	(%)		(kg/cm²)		(degree)	
HD-42	500	0.622	0.423	12.32	4.68	1104	42.4	13.6	0.242	868	3.21	31.7	0.000
HD-92	500	0.606	0.420	11.56	4.67	1166	41.0	14.3	0.231	889	3.33	32.5	0.000
HL-47	500	0.790	0.426	20.35	6.69	1190	37.2	13.4	0.249	897	3.38	32.9	0.000
HL-93	500	0.832	0.429	22.00	7.93	1197	40.0	14.9	0.232	899	3.39	33.0	0.000
HD-24	300	0.640	0.492	9.08	2.45	682	39.3	14.5	0.291	527	3.27	32.2	—
HD-90	300	0.602	0.479	7.62	2.36	713	41.0	15.1	0.272	538	3.38	32.9	0.057
HL-48	300	0.804	0.507	16.46	5.31	729	40.0	17.1	0.272	550	3.50	33.3	—
HL-91	300	0.819	0.497	17.68	5.65	762	43.0	17.2	0.259	554	3.54	34.0	0.048
HD-83	250	0.592	0.493	6.22	1.83	580	39.3	14.1	0.296	443	3.32	32.5	0.084
HD-80	200	0.596	0.509	5.41	1.69	460	37.0	13.3	0.319	353	3.30	32.4	0.106
HD-79	200	0.587	0.507	5.06	1.17	460	39.3	13.4	0.317	353	3.30	32.4	0.084
HL-81	200	0.820	0.577	13.39	3.69	470	47.0	19.1	0.303	357	3.35	32.8	0.075
HL-82	200	0.814	0.577	13.07	3.58	477	47.0	19.3	0.300	359	3.39	32.9	0.079
HD-78	175	0.593	0.520	4.61	1.55	393	41.2	12.9	0.335	306	3.25	31.9	0.088
HD-76	150	0.594	0.528	4.17	1.32	330	36.0	11.2	0.363	260	3.20	31.6	0.115
HL-77	150	0.843	0.643	10.80	2.71	347	48.0	19.4	0.353	266	3.31	32.4	0.070
HD-75	125	0.598	0.538	3.70	1.16	283	36.0	10.3	0.388	219	3.26	32.1	0.115
HL-74	125	0.846	0.672	9.60	2.38	283	47.5	19.3	0.379	219	3.26	32.1	0.104
HD-72	100	0.601	0.549	3.18	0.46	230.5	32.2	7.9	0.429	176.8	3.31	32.4	0.120
HD-73	100	0.609	0.556	3.22	0.62	228.0	33.0	8.2	0.438	176.0	3.28	32.2	0.115
HL-70	100	0.825	0.678	8.01	1.93	225.3	47.0	18.5	0.394	175.1	3.25	32.0	0.127
HL-71	100	0.832	0.686	7.96	1.54	228.2	47.5	18.7	0.399	176.1	3.28	32.2	0.127

Table 4. Results of triaxial tests at constant cell pressures on saturated samples.

Test No.	Confining pressure	Initial void ratio	Void ratio after compression	Volumetric strain due to compression	Axial strain due to compression	Values at the time of failure: Deviator stress	Axial strain	Volumetric strain	Void ratio	Mean normal stress	Principal stress ratio	Secant angle	Dilatancy rate
	(kg/cm²)			(%)	(%)	(kg/cm²)	(%)	(%)		(kg/cm²)		(degree)	
HD-68	75	0.597	0.550	2.90	0.86	176.0	27.0	5.3	0.472	134.6	3.38	32.7	0.115
HD-69	75	0.603	0.556	2.89	0.69	176.4	24.3	5.0	0.482	133.8	3.35	32.7	0.118
HL-65	75	0.824	0.713	6.08	1.16	169.8	42.4	16.4	0.454	131.6	3.26	32.1	0.136
HL-67	75	0.845	0.725	6.47	1.32	173.0	43.1	16.9	0.457	132.7	3.31	32.4	0.139
HD-63	50	0.609	0.569	2.45	0.54	124.5	13.4	1.4	0.547	91.5	3.49	33.7	0.040
HD-64	50	0.605	0.565	2.46	0.54	126.1	11.7	1.3	0.546	92.0	3.52	33.9	0.014
HL-61	50	0.819	0.723	5.28	0.77	109.0	33.0	10.5	0.545	86.3	3.18	31.4	0.139
HL-62	50	0.824	0.735	4.85	0.54	104.2	30.1	11.0	0.555	84.7	3.08	30.7	0.143
HD-55	25	0.611	0.578	2.10	0.31	77.1	8.9	−0.7	0.588	50.7	4.08	37.3	−0.162
HD-56	25	0.618	0.583	2.26	0.39	76.1	8.0	−0.6	0.593	50.4	4.04	37.1	−0.202
HL-58	25	0.795	0.735	3.35	—	62.3	21.0	4.5	0.659	45.8	3.49	33.7	0.075
HL-59	25	0.826	0.764	3.37	0.54	62.6	23.6	5.7	0.667	45.9	3.50	33.8	0.095
LD-16	5	0.627	0.616	0.75	0.35	17.6	3.9	−1.0	0.631	10.9	4.52	39.6	—
LD-21	5	0.616	0.605	0.77	0.39	16.9	4.0	−1.0	0.620	10.6	4.38	38.9	−0.554
LL-43	5	0.830	0.784	2.52	1.18	11.8	8.0	0.5	0.775	8.93	3.36	32.8	−0.104
LL-44	5	0.831	0.796	1.88	0.65	11.8	8.3	0.5	0.787	8.93	3.36	32.8	—
LD-10	3	0.622	0.613	0.57	0.16	11.4	4.3	−1.4	0.636	6.80	4.80	40.9	−0.674
LD-11	3	0.624	0.608	1.03	0.15	11.3	4.6	−1.5	0.631	6.77	4.77	40.8	—
LL-45	3	0.817	0.793	1.35	0.57	6.99	6.1	0.0	0.793	5.33	3.33	32.6	—
LL-46	3	0.816	0.785	1.71	0.65	7.00	7.3	0.3	0.779	5.33	3.33	32.6	−0.068
LD- 2	1	0.604	0.600	0.25	—	4.01	3.2	−1.6	0.625	2.33	5.00	41.9	—
LD- 4	1	0.609	0.604	0.27	—	4.21	4.9	−1.9	0.634	2.40	5.20	42.7	−0.747
LL-48	1	0.839	0.821	1.01	0.32	2.40	4.0	0.2	0.816	1.80	3.40	33.1	—
LL-49	1	0.832	0.812	1.08	0.32	2.41	4.9	0.2	0.809	1.80	3.40	33.1	−0.078

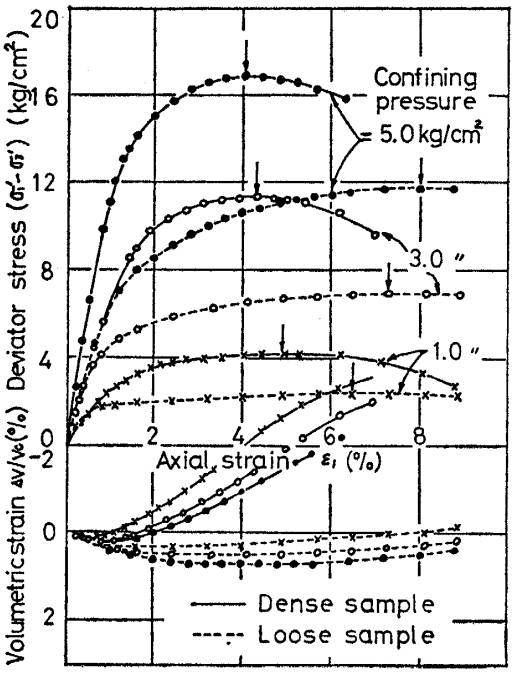

Fig. 11. Typical results of standard triaxial tests at low pressures.

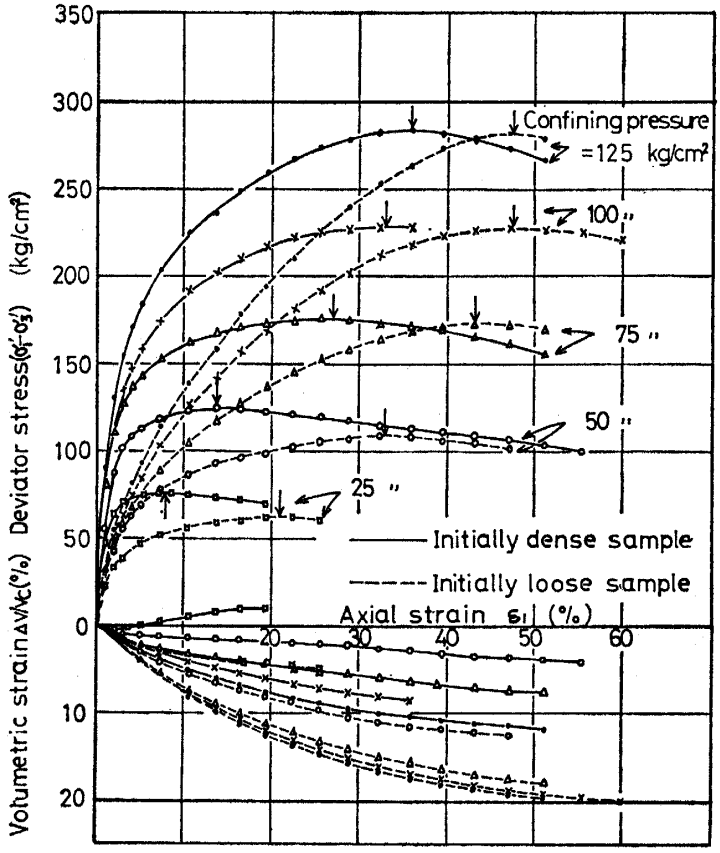

Fig. 12. Stress-strain curves of saturated samples at elevated cell pressures.

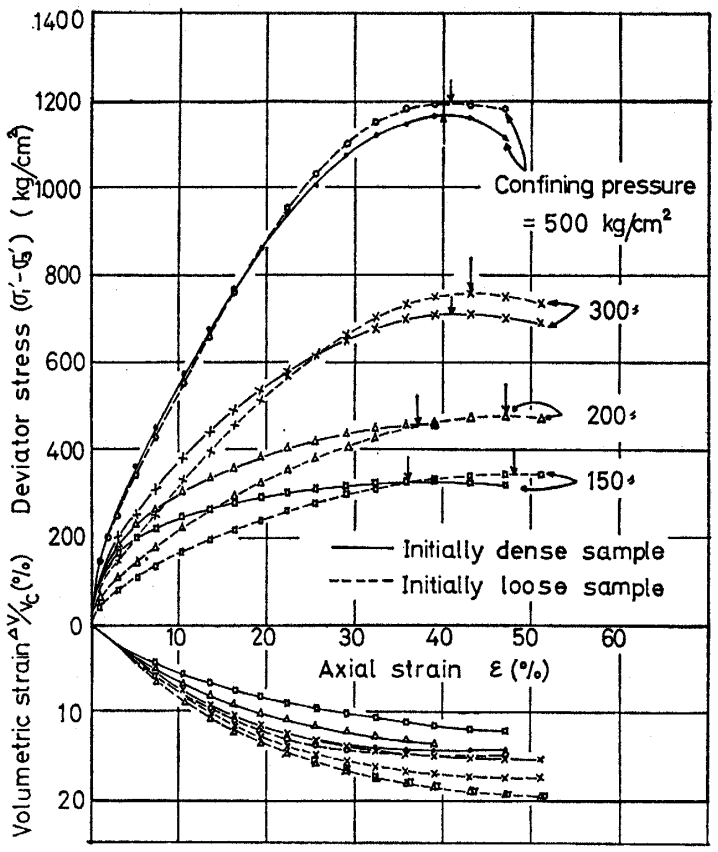

Fig. 13. Stress-strain curves of saturated samples at high pressures.

discussions of the magnitude of the shear strength components in the two samples can be made with the aid of the expression proposed by Lee and Seed[3]:

$$\tau = \tau_s + \tau_d + \tau_c \qquad \cdots\cdots\cdots(3)$$

where, τ is the measured strength, τ_s strength due to sliding friction, τ_d dilatancy effect, and τ_c crushing and rearranging effects. In the following discussions, the suffices D and L indicate the dense state and loose state of the samples, respectively, and the numeral indicates the magnitude of the confining pressure. At the time of failure of the samples, which were sheared at a confining pressure of 75kg/sq. cm, the measured shear strength of the dense state sample τ_{D75} was nearly equal to that of the loose state sample τ_{L75}, as shown in Table 3. Provided that τ_s is affected only by normal stress, then τ_{sD75} can be considered to be approximately equal to τ_{sL75}. Besides that, the dilatancy rates $dv/d\varepsilon$ at failure were 0.115 and 0.136 for the dense and loose samples, respectively. By substituting these conditions into Eq. (3), it is seen that the value τ_{cL75} is larger than the value τ_{cD75}. In other words, the difference in the dilatancy effect between the two samples was supplemented by the difference in the crushing and rearranging effects and, hence, the maximum deviator stresses were approximately the same.

The effect of initial porosity on the stress-strain relationships decreased with increasing confining pressures, as can be seen in Fig. 13. However, even at such a high pressure as 500 kg/sq. cm, the initial porosity continued to influence the stress-strain relationships. The examinations of the shear strength components at the time of failure were made on the samples which were deformed at the confining pressure of 500 kg/sq. cm, as follows: As before, the shear strength of the initially loose state sample τ_{L500} was larger than that of the initially dense one τ_{D500}, as is seen in Table 3. Furthermore, the dilatancy and rearranging effects of both samples, τ_{dD500} and τ_{dL500}, were the same because their values of $dv/d\varepsilon$ at the time of failure were both zero. Accordingly, it was also found that the value of τ_{cL500} was larger than that of τ_{cD500}. Thus, for the samples under consideration, it can be said that the initially loose state sample mobilized a larger maximum deviator stress than the initially dense state one by a magnitude resulting from the difference in the energies dissipated in crushing and rearranging the sand grains.

At very high pressures, the effect of initial porosity on the shear characteristics of a sand may disappear.

Mohr diagrams of the samples tested are given in Fig. 14. In the lower pressure range, the Mohr envelopes for both dense and loose samples are straight, whose gradients are 40.6 and 33.0 degrees respectively, and they tend towards the origin of the diagram. The envelope for the dense samples, however, deviates from the straight line with an increase in the normal pressure. This tendency can be considered to indicate the disappearance of the phenomenon producing the dilatancy effect as the confining pressure increases. The Mohr envelopes for a wider range of normal pressures are presented in Fig. 14(b) and (c).

The secant angle of shearing resistance of each sample was calculated using the following equation:

$$\phi_s = \sin^{-1}\frac{\sigma_1-\sigma_3}{\sigma_1+\sigma_3} \qquad \cdots\cdots\cdots(4)$$

where, σ_1 and σ_3 are the major and minor principal stresses, respectively. The values calculated for the secant angle of shearing resistance are given in Tables 3 and 4, and the curves of the secant angle as a function of the confining pressure are presented in Fig. 15. It can be seen from this diagram that the values of ϕ_s for the loose state samples are nearly constant for the various confining pressures, while for the dense state samples ϕ_s decreases with increasing of confining pressure until this curve coincides with that of the loose state sample. Since similar relationships have been found in another investigation[4], it may be stated that: the angle of shear resistance of a sand under very high confining pressures can be estimated approximately from the angle of shear resistance of a very loose state of the same sand under low confining pressures, because the dilatancy effect of the dense sample will disappear under high pressures.

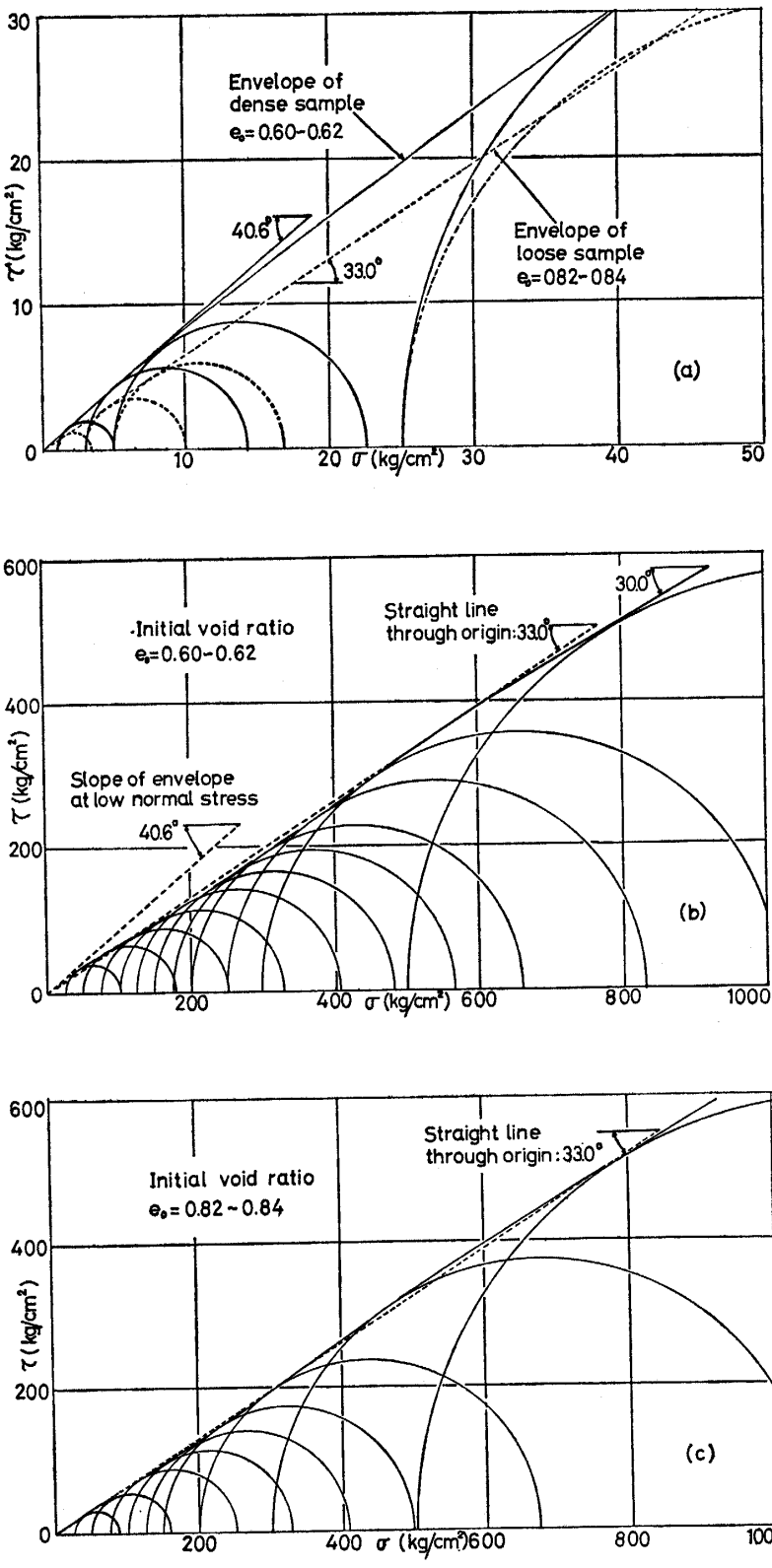

Fig. 14. Mohr diagrams.

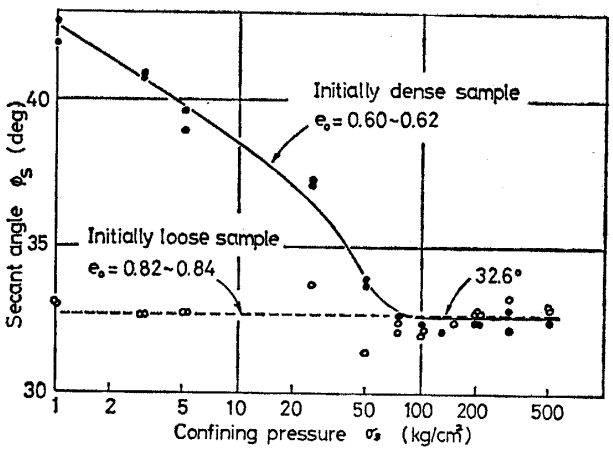

Fig. 15. Relationship between secant angle of shearing resistance and confining cell pressure.

In order to study the effect of pore water on the shear characteristics of a sand, a series of drained shear tests were conducted on desiccator-dried sand. The relationships between deviator stress, axial strain (natural) and volumetric strain (natural) on the initially dry dense samples are shown in Figs. 16 and 17, which, for comparison, contain the similar relationships on the initially

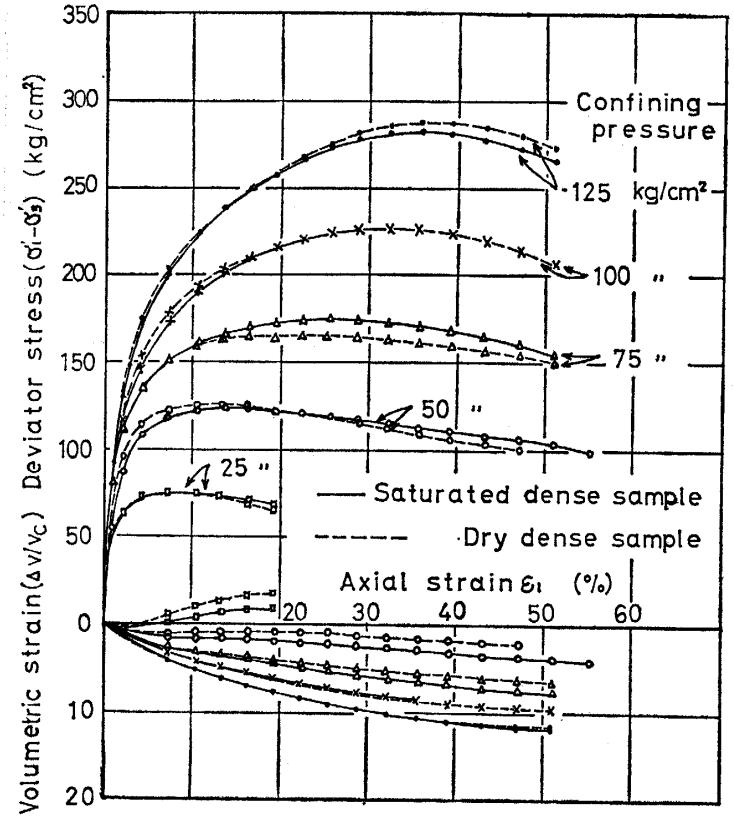

Fig. 16. Comparisons of stress-strain curves between saturated and dry samples at elevated cell pressures.

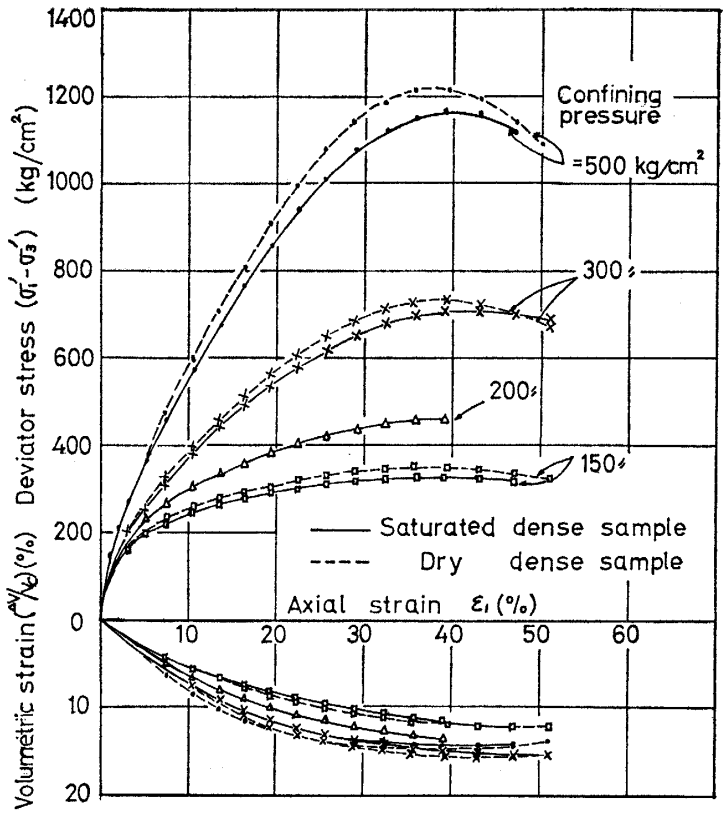

Fig. 17. Comparisons of stress-strain curves between saturated and dry samples at high pressures.

saturated dense samples. The shear characteristics of the dry samples are distinguished from those of the saturated ones in the following aspects: The deviator stresses on the dry samples at confining pressures higher than 125 kg/sq. cm were greater than those for the saturated ones at any level of axial strain. The volume contraction of the dry sample during shear was smaller than that of the saturated one at confining pressures up to 100 kg/sq. cm, and *vice versa* at confining pressures higher than 250 kg/sq. cm.

The gradings of the sheared samples are given in Table 5. It is evident that the crushing effects in dry samples are larger than those in saturated ones, when the samples are sheared at confining pressures higher than 300 kg/sq. cm. This difference must be related to the difference in volume contractions between the dry and saturated samples, as previously described. At confining pressures up to 100 kg/sq. cm, the amount of grain crushing in the dry sample was smaller than in the saturated sample. Since the interparticle friction angle was assumed to be affected by the existence of water, and also since the amount of this is not known, any examination of the shear strength components could not be made.

From an observation of the sheared specimens, it was found that a predominant shear failure plane was present in all of the dry samples, although traces of multiple failure planes were found on the inner wall of the rubber membrane. In the saturated samples which were sheared at the confining pressures higher than

Table 5. Gradings of the samples after triaxial tests.

Test No.	Confining pressure (kg/cm²)	Initial Density	Moisture Condition	Shear Strain* (%)	Per cent finer by weight								
					250μ	177μ	149μ	105μ	74μ	50μ	30μ	10μ	5μ
HD- 92	500	Dense	Sat**	51.1	—	86.5	70.2	64.5	60.6	47.3	37.8	19.2	10.8
HL- 93	500	Loose	Sat	47.0	—	88.4	72.2	66.3	61.9	50.0	39.5	20.0	12.0
HD-126	500	Dense	Dry	51.1	98.9	87.8	79.2	69.3	61.1	54.0	44.7	25.0	15.0
HD- 90	300	Dense	Sat	51.1	99.0	85.5	66.0	59.7	54.6	42.5	32.5	15.8	9.6
HL- 91	300	Loose	Sat	51.1	99.1	86.1	67.4	60.9	55.3	43.0	33.2	16.0	9.8
HD-125	300	Dense	Dry	51.1	99.0	84.0	73.2	62.2	53.4	45.6	36.0	20.2	11.2
HD- 79	200	Dense	Sat	49.5	—	77.6	63.4	49.1	39.0	31.9	24.0	12.0	7.2
HL- 81	200	Loose	Sat	51.1	—	78.5	66.1	52.3	42.3	36.0	26.5	13.0	7.0
HD- 72	100	Dense	Sat	51.1	97.2	68.0	48.8	37.4	30.0	22.0	15.1	7.8	5.2
HL- 70	100	Loose	Sat	53.0	97.1	69.2	50.3	38.8	31.1	24.8	18.1	8.8	5.4
HD-119	100	Dense	Dry	51.1	97.0	62.6	46.9	35.2	27.4	22.3	17.7	10.3	7.0
HL-153	100	Loose	Dry	51.1	98.2	70.2	54.9	43.0	36.1	17.0	12.1	7.0	3.3
HD- 68	75	Dense	Sat	51.1	97.3	62.0	41.2	32.1	24.8	19.5	13.9	6.6	4.5
HL- 65	75	Loose	Sat	51.1	97.0	—	—	32.9	25.4	21.0	15.9	7.0	4.6
HD-116	75	Dense	Dry	51.1	95.8	53.4	37.3	27.0	20.4	16.2	12.5	7.8	6.2
HL-150	75	Loose	Dry	51.0	95.7	57.6	38.1	25.5	18.2	—	—	—	—
HD- 63	50	Dense	Sat	55.0	95.8	—	31.4	21.9	16.2	—	—	—	—
HL- 60	50	Loose	Sat	51.1	95.1	—	29.5	19.9	14.7	—	—	—	—
HD-115	50	Dense	Dry	47.7	95.3	45.8	25.8	16.5	11.2	—	—	—	—
HL-149	50	Loose	Dry	51.0	95.6	50.0	27.6	16.4	10.9	—	—	—	—

* Natural strain. ** Sat: Saturated.

250 kg/sq. cm, however, no predominant shear failure plane appeared. Hence, it may be said that a saturated sample deforms more plastically than a dry sample when it is compressed under high confining pressures. These differences in macroscopic behavior between the two samples may be explained by such microscopic phenomenon at the contact parts of the grains as, for example, the dissolution of silica into pore water or the action of water which is enclosed by surrounding asperities at the contact parts of adjacent grains. If this is the case, then the pore water will act as a kind of lubricant and decrease the interparticle friction.

In order to understand how the bond formation developed between particles under high pressures, several unconfined compression tests and slaking tests

were conducted on the sheared samples. The results of the unconfined compression tests are shown in Table 6. After the unconfined compression tests, the samples were dried in an oven for 24 hours, and then some broken pieces of a sample were put into a beaker which was filled with water. The pieces of the initially dry dense sample, which had been sheared at a confining pressure of 500 kg/sq. cm, disintegrated into a granular state within one minute. On the other hand, the pieces of the initially saturated loose sample, for which confining pressure had also been 500 kg/sq. cm, retained their original shapes when placed in water even for 24 hours, although a little part of pieces crumbled off. These results indicate that some kind of bond formation had developed at the contact parts of the grains under high intergranular pressure with the help of water action.

Table 6. Unconfined compression strength of the samples after shear tests.

Test No.	Moisture condition at shear	Initial density	Confining pressure (kg/cm^2)	Comprssion strength (kg/cm^2)	Storage time* (days)
HD-126	Dry	Dense	500	0.4	0
HD- 4	Sat**	Dense	500	9.3	750
HL- 49	Sat	Loose	500	4.2	700
HD- 45	Sat	Dense	300	2.0	695
HL- 29	Sat	Loose	300	0.7	730

* The samples were kept in a moist box after shear tests.

** Sat: Saturated.

Conclusions

In order to investigate the mechanical properties of a sand subject to high confining pressures, a series of drained shear tests were performed on so-called "Toyoura standard sand." At such elevated isotropic pressures as 175 kg/sq. cm, a particular relationship was found between degree of compression, isotropic pressure and compression time, from which the time required for 100 per cent compression can be estimated. It was also found that the greater part of grain crushing had been attained until the initial reflection point, which occurred in the curves of the degree of compression as a function of the logarithm of the compression time. Under high isotropic pressures, the compressibility of the sand was affected significantly by the action of pore water. The porosity of a sand at high pressures was found to be affected not only by the magnitude of the compression pressure but also by its duration.

A comparative discussion of the magnitude of the shear strength components was made for the two samples which were initially of different porosities. For the samples sheared at the confining pressure of 75 kg/sq. cm, it was found that at the time of failure the difference in the dilatancy effects between the

two samples, one initially dense and the other initially loose, was compensated for by the difference in the crushing and rearranging effects, so that the maximum deviator stresses were approximately the same. For the two samples for which the confining pressure was 500 kg/sq. cm, it was also found that the initially loose state sample mobilized a larger maximum deviator stress than the initially dense state one by a magnitude resulting from the difference between the energies dissipated in crushing and rearranging the sand grains. Thus, the initial porosity affects the shear characteristics of the sand even at such a high confining pressure as 500 kg/sq. cm. It can be said that the shear characteristics of a sand under high pressure are strongly related to the crushing strength of the grains. Under high confining pressures, pore water also influenced significantly the shear characteristics of the sand, such as the stress-strain relationship, the volume contraction and the amount of grain crushing during shear. The sand specimens under high pressures deformed more plastically as a result of water action. It is noted that some kind of bond formation developed at contact parts of the grains under high intergranular pressures with the help of pore water action.

References

1) Bishop, A. W. and Henkel, D. J., "The Measurement of Soil Properties in the Triaxial Test.", Edward Arnold Ltd., London, Second edition, (1962).
2) Rowe, P. W., "The Stress-dilatancy Relation for Static Equilibrium of an Assembly of Particles in Contact.", Proc. Roy. Soc., A 269, 500–527, (1962).
3) Lee, K. L. and Seed, H. B., "Drained Strength Characteristics of Sands.", Proc. ASCE, Vol. 93, No. SM 6, 117–141, (1967).
4) Vesic, A. S. and Clough, G. W., "Behavior of Granular Materials under High Stresses.", Proc. ASCE, Vol. 94, No. SM 3, 661–688, (1968).